Journal of Applied Physics ARTICLE scitation.org/journal/jap

Dark current analysis of germanium-on-insulator vertical *p-i-n* photodetectors with varying threading dislocation density

Cite as: J. Appl. Phys. **127**, 203105 (2020); doi: 10.1063/5.0005112
Submitted: 21 February 2020 · Accepted: 11 May 2020 ·
Published Online: 27 May 2020

Bongkwon Son,[1,a)] Yiding Lin,[1,2] Kwang Hong Lee,[2] Qimiao Chen,[1] and Chuan Seng Tan[1,2]

AFFILIATIONS

[1]School of Electrical and Electronic Engineering, Nanyang Technological University, 50 Nanyang Avenue, Singapore 639798
[2]Low Energy Electronic Systems (LEES), Singapore-MIT Alliance for Research and Technology (SMART), Singapore 138602

[a)]**Author to whom correspondence should be addressed:** BONGKWON001@e.ntu.edu.sg

ABSTRACT

Dark current characteristics of germanium (Ge) vertical *p-i-n* photodetectors were studied. Ge photodetectors were demonstrated on the germanium-on-insulator (GOI) platforms realized via direct wafer bonding and layer transfer. GOI platforms with two different threading dislocation densities (TDDs) of $3.2 \times 10^6\,\mathrm{cm}^{-2}$ (low TDD) and $5.2 \times 10^8\,\mathrm{cm}^{-2}$ (high TDD) were varied via furnace annealing in oxygen ambient. An ultra-low dark current density of $1.12\,\mathrm{mA/cm}^2$ for epi-Ge photodetectors was obtained for a low TDD Ge photodetector. This is reduced by a factor of 53 in comparison with a high TDD Ge photodetector. A dominant leakage contribution component shifts from bulk leakage to surface leakage as TDD decreases to $3.2 \times 10^6\,\mathrm{cm}^{-2}$, suggesting that advanced surface passivation is required to further reduce the leakage current. Through an activation energy study, it is revealed that a primary bulk leakage mechanism shifts from Shockley–Read–Hall (SRH) leakage to diffusion leakage in a temperature range of 323–353 K. The surface leakage performed with plasma enhanced chemical vapor deposition-deposited SiO_2 is governed by SRH and trap-assisted tunneling leakage processes. Two orders of magnitude enhancement in the effective carrier lifetime is observed with the reduction in TDD. This work suggests that bulk leakage current density and effective lifetime analysis provide a better understanding of TDD-dependent dark leakage current study.

I. INTRODUCTION

A germanium (Ge) photodetector (PD) is one of the key building blocks for Si-based integrated photonics. The main research focus has been for high speed, wide bandwidth, and high responsivity, taking advantage of complementary metal-oxide-semiconductor (CMOS)-compatibility and the considerable absorption coefficient at the near-infrared (near-IR) range.[1–3] However, Ge photodetectors suffer from high dark leakage current, which has been reported orders of magnitude higher than that of InGaAs photodetectors. Ge *p-i-n* diodes have been revealed to display $\sim 10\,\mathrm{mA/cm}^2$ of dark current density, in contrast to $\sim 0.5\,\mu\mathrm{A/cm}^2$ for InGaAs *p-i-n* photodetectors.[4,5] This critical drawback of Ge photodetectors brings performance degradation in terms of detectivity, noise equivalent power (NEP), and responsivity.

The leakage current on Ge photodetectors has been reported to mainly originate from misfit dislocations and threading dislocations formed in epitaxial Ge layers.[5,6] These dislocations, generated due to about 4% lattice mismatch between Ge and Si, act as electrical tunneling and generation trap centers. The generation of minority carriers through dislocated-trap centers in Ge, called as a Shockley–Read–Hall (SRH) process, has been proposed as the dominant leakage current mechanism for Ge photodetectors.[6–8] In addition, the electrical tunneling of minority carriers through dislocated-trap centers, called as a trap-assisted tunneling (TAT) process, further enhances leakage current in high reverse bias.[6,7] These two leakage current mechanisms, SRH and TAT leakages, not only block suppression on leakage current, but also restrict huge current variation under different operating temperatures. Therefore, the study on leakage current dependence on dislocations in epitaxial Ge layers is important to improve Ge photodetector performance.

The leakage current has been widely associated with the amount of threading dislocation density (TDD) for Ge photodetectors and for shallow Ge *pn* junctions.[6–10] Tremendous efforts have been made to decrease dark currents of Ge *p-i-n* diodes and p^+/n junctions by

reducing TDDs of Ge layers. The dark current density for Ge p^+/n junctions with the TDD of 4.2×10^8 cm^{-2} was reduced by roughly 10× compared to the one with the TDD of 1.6×10^{10} cm^{-2}.[5] The dark current of Ge *p-i-n* photodiodes with the TDD of $\sim 5 \times 10^7$ cm^{-2} was reduced by 45× from the one with the TDD of $\sim 3 \times 10^8$ cm^{-2}.[8] Ge p^+/n junctions with the TDD of ~ 1–2×10^7 cm^{-2} show the dark current of roughly 5× and 25× lower than the one with the TDD of $\sim 4 \times 10^8$ and $\sim 2 \times 10^{10}$ cm^{-2}, respectively.[11] Furthermore, a germanium-on-insulator (GOI) substrate has been demonstrated with TDD as low as $\sim 10^6$ cm^{-2} via direct wafer bonding (DWB) and layer transfer followed by the oxygen (O_2) annealing process, taking advantages of wafer-scale fabrication and back-end-of-line (BEOL) integration.[12,13] However, the dark current study on such low TDD Ge photodetectors is still lacking.

In this paper, the dark current of vertical *p-i-n* Ge photodetectors (PDs) with two different TDDs of 3.2×10^6 cm^{-2} (low TDD) and 5.2×10^8 cm^{-2} (high TDD), is analyzed and compared. GOI platforms are introduced for device demonstrations via DWB and layer transfer techniques. To vary the TDD in epitaxial Ge layers, the additional O_2 annealing process is conducted. The leakage current of Ge PDs is reduced by 53× as TDD decreases by two orders of magnitude accordingly. The dominant leakage current contribution shifts from bulk leakage to surface leakage by reducing the TDD in the GOIs. The extracted surface leakage current constitutes 96% of the total leakage current for low TDD Ge PDs, indicating that advanced surface passivation would further reduce the leakage current. Through an activation energy (E_a) study, it is confirmed that the key bulk leakage mechanism of Ge PDs shifts from SRH leakage to the diffusion leakage process as the TDD decreases in the temperature range of 323–353 K. Besides, the effective carrier lifetime (τ_{eff}) for low TDD Ge PDs shows two orders of magnitude higher value than that for high TDD Ge PDs. It is confirmed that bulk leakage and τ_{eff} are significantly affected by reduction in TDD. This dark current analysis through various characteristic analysis methods expends the interpretation of Ge photodetector characteristics and their dependence on TDD.

II. VERTICAL GE *p-i-n* PHOTODETECTORS DARK CURRENT ANALYSIS

A. Demonstration of vertical *p-i-n* photodetectors on GOI platforms

200 mm GOIs were realized via direct wafer bonding and layer transfer techniques, as described in Ref. 12. The silicon dioxide (SiO_2) and silicon nitride (SiN) layers were inserted as the intermediate layers to form GOI. The GOI substrate was subjected to the O_2 annealing process at 850 °C for 4 h to reduce the TDD in epitaxial Ge layers.[12] The etched-pit density (EPD) was extracted to estimate the defect density in GOI. As shown in Fig. 1(a), EPD of the O_2-annealed Ge layer was 3.2×10^6 cm^{-2}, indicating that the TDD of the O_2-annealed Ge layer was dramatically reduced compared to that of the unannealed Ge layer, 5.2×10^8 cm^{-2}, as the previous study was reported.[12] It is worth noting that two orders of magnitude TDD reduction in Ge was achieved through direct wafer bonding and layer transfer techniques followed by O_2 anneal.[12] In addition, thickness of Ge films is reduced by ~300 nm during O_2 annealing and HF solution etching processes.

With boron (B) ion implantation on epitaxial Ge layers on Si before bonding, and with arsenic (As) ion implantation after the formation of GOI, a vertical *p-i-n* diode was formed. Figure 1(b) displays a secondary ion mass spectroscopy (SIMS) image of the As and B doping concentration profiles for the low TDD Ge *p-i-n* structure. Heavily *p*+- and *n*+-doped regions of both As and B doping concentration were achieved in shallow doping depth. Heavily doped regions on top and bottom in Ge were introduced for ohmic contact formation. The vertical Ge photodetectors were then demonstrated on GOI platforms with two different TDDs, i.e., 3.2×10^6 and 5.2×10^8 cm^{-2}, respectively, referring to the process flow in Ref. 14. The p^+- and n^+-mesas were formed by Cl_2-based reactive ion etching (RIE). Ge photodetector mesas with diameters of 60, 80, 150, and 250 μm were designed and fabricated. Surface passivation was performed with a deposition of a 400-nm SiO_2 layer by plasma enhanced chemical vapor deposition (PECVD). Metal contact holes were exposed via the combination of CF_4-based RIE and buffered oxide etching (BOE). Ti/TiN/Al layers were deposited by sputtering, followed by a rapid thermal annealing (RTA) process for 1 min at 400 °C to enhance the ohmic contact. A planar-view SEM image of the photodetector with a 250 μm diameter is shown in Fig. 1(c). The top-center electrode is connected with the n^+-mesa on the top of Ge, and both side electrodes are connected with the p^+-mesa in the bottom Ge. A 3D schematic image of the completed vertical *p-i-n* photodetector is shown in Fig. 1(d). The thicknesses of low and high TDD Ge PDs are 1.1 and 1.4 μm, respectively.

B. Vertical *p-i-n* Ge photodetector performance

Dark current density–voltage (J_{dark}–V) curves of vertical *p-i-n* photodetectors on low and high TDD GOI substrates are summarized in Fig. 2(a) with varying Ge mesa diameters ranging from 60 to 250 μm. J_{dark} for high TDD Ge PDs with a 250 μm diameter was measured as 59.49 mA/cm^2 at −1 V. J_{dark} for low TDD Ge PDs was measured as 1.12 mA/cm^2 and increased to 3.96 mA/cm^2 by decreasing the PD diameters from 250 to 60 μm. It should be noted that J_{dark} is reduced by 53× as TDD is reduced from 5.2×10^8 to 3.2×10^6 cm^{-2}. Diode ideality factors were extracted from forward J_{dark}–V characteristics as 1.70 and 1.23 for high and low Ge PDs, respectively. The diode ideality factor is reduced by 0.47 for low TDD Ge PDs, indicating the reduced carriers trapping effects due to fewer defect states in low TDD Ge PDs.

Temperature-dependent dark current–voltage (I_{dark}–V) curves for low and high TDD Ge PDs with a 250 μm diameter were measured in the temperature range from 293 to 353 K in Fig. 2(b). I_{dark} for a high TDD Ge PD was measured as 29.2 μA at 293 K under −1 V and increased by 10.9× at 353 K. For a low TDD Ge PD, I_{dark} was measured as 548 nA at 293 K and increased by 12.4× at 353 K. The elevating leakage current in the temperature variation is enhanced for low TDD Ge PD. This is because of the alleviation of dislocations in Ge. I_{dark} for the low TDD Ge photodetector with a 60 μm diameter was measured as 122 nA at 293 K and increased by 10.7× at 353 K under −1 V (not shown). The elevating leakage current in the temperature variation is reduced as the size of low TDD Ge PDs decreases.

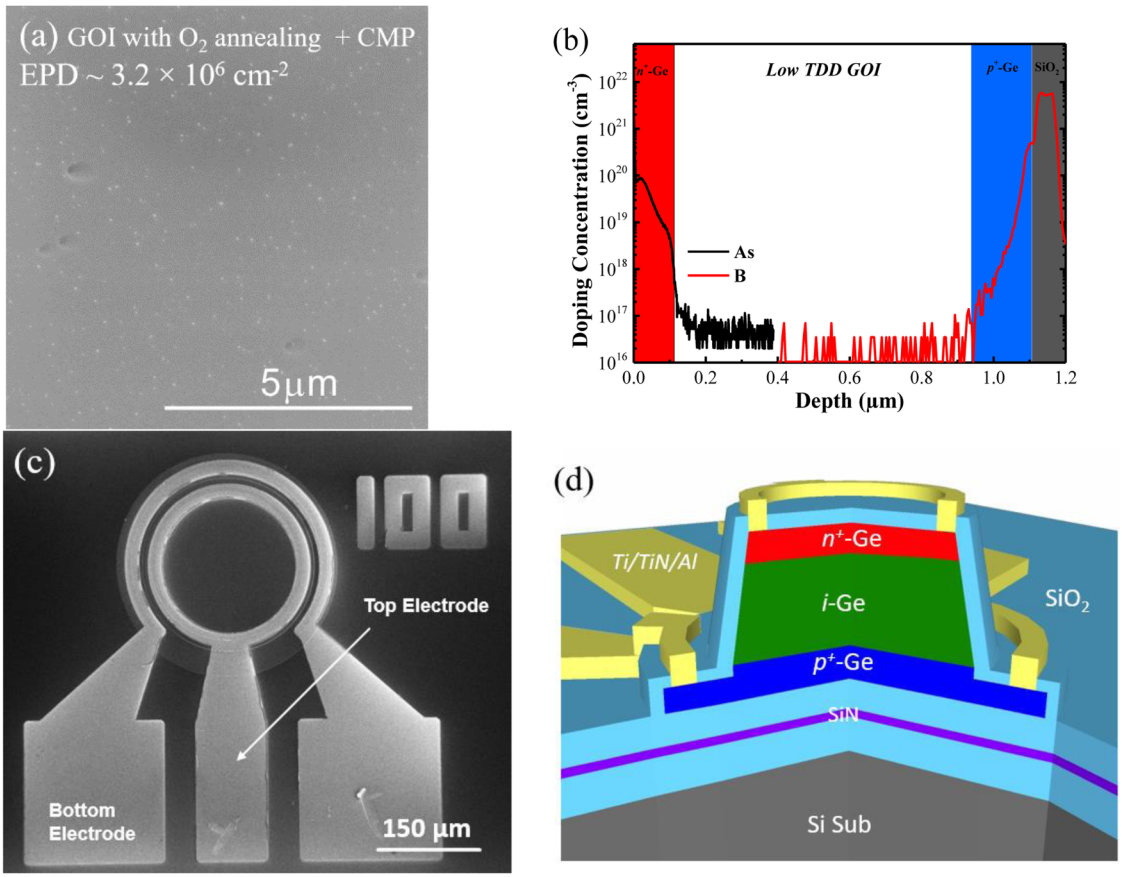

FIG. 1. (a) A SEM image of low TDD GOI via the O_2 annealing process. EPD is estimated to be 3.2×10^6 cm^{-2}. (b) Doping concentration profiles of the vertical *p-i-n* low TDD GOI structure via SIMS analysis. The Ge layer is formed with a ~1.1 μm thickness. (c) Planar-view SEM and (d) 3D schematic images of a vertical *p-i-n* Ge photodetector.

The inset in Fig. 2(c) shows photocurrent response for low and high TDD Ge photodetectors at 1550 nm. Responsivity for low and high TDD Ge photodetectors was revealed to be 0.24 and 0.41 A/W at −1 V, respectively. The responsivity is reduced for the low TDD Ge PD, originating from Ge thickness reduction during O_2 annealing and HF solution etching. Photo-response performance can be normalized with responsivity per unit of depletion thickness, as shown in Fig. 2(b). The decrease in responsivity with increasing reverse bias is observed due to the strong Franz–Keldysh effect. Photo-response performance is enhanced for the reverse bias of <1.3 V, whereas it is degraded for the reverse bias of >1.3 V compared to the high TDD Ge photodetector due to a relatively strong electric field applied in a depletion region for a low TDD Ge photodetector.

C. Dark current analysis

In order to further investigate the leakage current, it is important to attribute it to two leakage current components, i.e., a surface leakage current (I_{surf}) and a bulk leakage current (I_{bulk}).[15] I_{surf} is the leakage current originated from minority carrier generation and flows on the Ge layer sidewall due to poor surface passivation. The unstable bonds such as dangling bonds generate surface defect states at the interfaces. In this work, since the PECVD-deposited SiO_2 passivation layer is not the perfect surface layer to eliminate surface/interface states, the leakage current is generated and flows through the surface defect states formed on the sidewall of Ge PDs. Thus, the sidewall in intrinsic Ge layers is only considered for I_{surf}, since heavily doped regions are formed by As and B ion implantation on the top and bottom GOI, respectively. I_{bulk} is the leakage current originated from minority carrier generation and flows in the neutral and depletion regions. Several reports on Ge *p-i-n* PDs have discussed the role of dislocations in the epi-Ge layer that serve as intermediate states, referred to as Shockley Read centers.[6–8] These defects states enhance the generation of minority carriers through trap states, which is the dominant leakage current mechanism in Ge PDs with high TDD.[16] Besides, the leakage current can be enhanced by the TAT leakage process.[16]

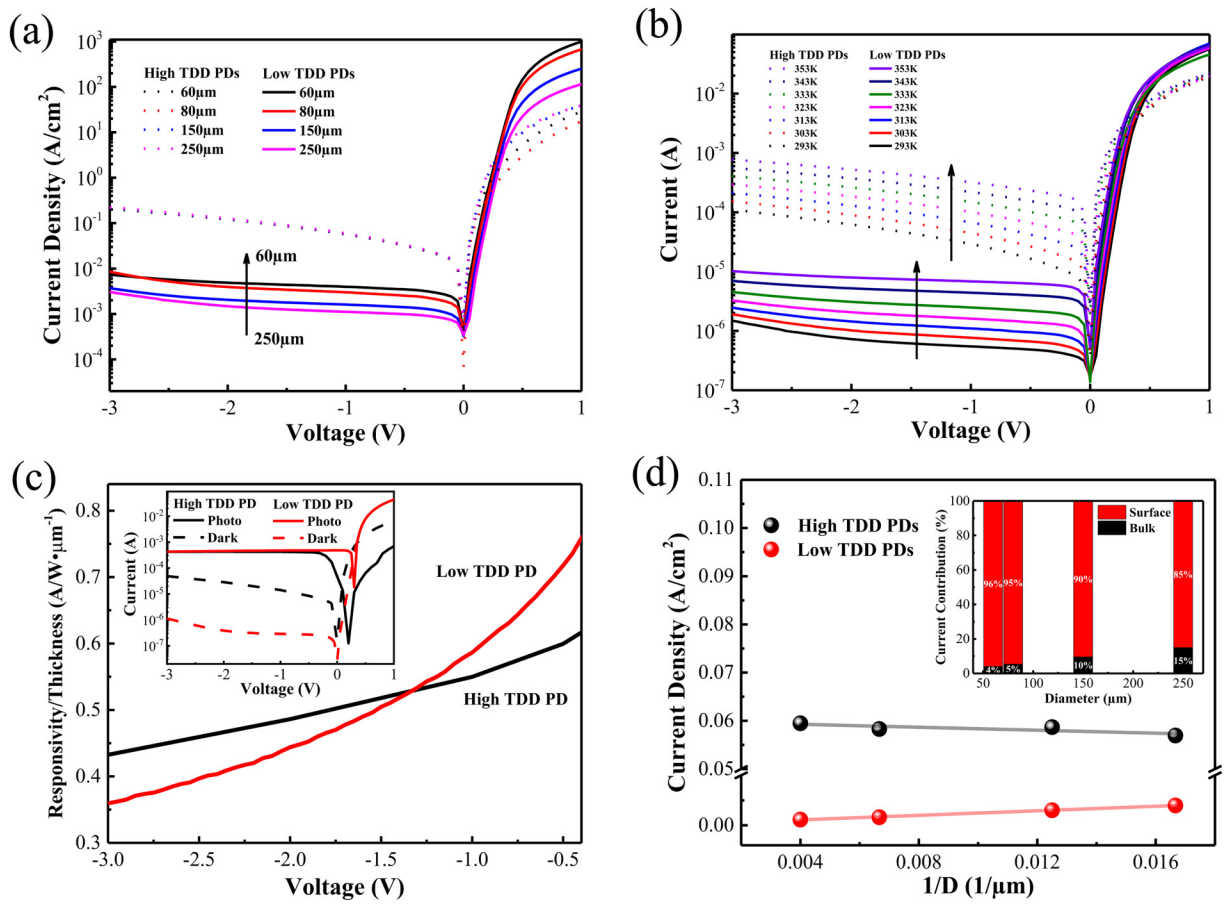

FIG. 2. (a) The dark current density–voltage (J_{dark}–V) characteristics for low and high TDD Ge photodetectors with varying Ge mesas. (b) Temperature-dependent dark current (I_{dark}) for the low TDD Ge photodetector in comparison with the one for high TDD PD with a 250 μm diameter as a function of voltage. The arrows represent the temperature increasing from 293 to 353 K. (c) The thickness-normalized responsivity performance for low and high TDD Ge photodetectors at 1550 nm wavelength. The inset displays the photocurrent–voltage (I_{photo}–V) curve for low and high TDD Ge photodetectors. (d) J_{dark}–$1/D$ characteristics for the low and high TDD Ge photodetectors at −1 V at 293 K. Inset displays current contribution of the bulk and surface leakage for low TDD Ge photodetectors with varying Ge mesas.

The surface and bulk leakage current densities can be expressed by the following equation:

$$J_{dark} = J_{bulk} + J_{surf} \times \frac{4}{D}, \quad (1)$$

where J_{bulk} and J_{surf} are the bulk and surface leakage current densities, respectively, and D is the diameter of a Ge PD.[17] Both J_{surf} and J_{bulk} can be extracted from the linear relationship between J_{dark} and $1/D$. Figure 2(d) displays J_{dark} for low and high TDD Ge PDs with diameters of 60, 80, 150, and 250 μm at −1 V as a function of $1/D$. J_{bulk} is extracted as 0.16 and 59.92 mA/cm^2 for low and high TDD Ge PDs, respectively. The J_{surf} for low TDD Ge PDs was extracted to be 5.67 μA/cm. The J_{surf} for high TDD Ge PDs is considered as negligible because J_{surf} is extremely low compared to J_{bulk}.[14] Such extremely suppressed J_{bulk} for low TDD Ge PDs can be explained with two reasons. First of all, TDD reduction in the Ge layer from 5.2×10^8 to 3.2×10^6 cm^{-2} provides fewer trap centers in the depletion region of Ge *p-i-n* diodes. Thus, much smaller trap density in low TDD Ge reduces SRH and TAT leakage currents accordingly. Second of all, as the consequence of O_2 anneal and HF solution etching, the relatively thin 1.1 μm thickness of the low TDD Ge layer provides a short distance for minority carriers to pass through the depletion region compared to the 1.4 μm thick high TDD Ge layer. The depletion width is the important parameter to determine the influence of SRH and TAT processes on the leakage current because either SRH or TAT leakage currents are proportional to depletion width.[7] Thus, the thin depletion region in low TDD Ge suppresses the SRH and TAT processes.

The inset in Fig. 2(d) displays a leakage current contribution of bulk and surface leakage for low TDD Ge PDs at −1 V as a function of photodetector diameters. The current contribution for high TDD Ge PDs is not shown since the bulk leakage current contribution is ~100% regardless of device size. The bulk leakage contribution of

only 4% was obtained for the low TDD Ge PD with a 60 μm diameter, whereas the leakage current of 96% is contributed by surface leakage, indicating that a surface leakage mechanism has to be considered as the primary leakage current component for Ge with such low TDD of 3.2×10^6 cm^{-2}. It should be noted that Ge PDs with the TDD of $\sim 10^8$ cm^{-2} show the bulk leakage current dominance. However, as TDD reaches $\sim 10^6$ cm^{-2}, the key leakage current contribution shifts to surface leakage. It has been reported that Ge PDs with the TDD of $\sim 5 \times 10^7$ cm^{-2} was contributed mainly by surface leakage for $10 \times 10\,\mu$m^2 size.[8] The surface leakage current contribution increases with decreasing the diameter of PDs since the smaller device has a greater perimeter to area ratio than that of larger ones. The surface current contribution of a low TDD Ge photodetector increases from 85% to 96% as the diameter decreases from 250 to 60 μm. This result points out the necessity of advanced surface passivation for low-TDD Ge PDs, especially for the devices with diameters of a few tens of micrometers. As advanced surface passivation, GeO_x surface passivation is attractive to suppress surface leakage, taking advantage of the high-k dielectric property and low intermediate surface defect states.[18] Thin GeO_x layer has been introduced with thermal annealing, Oxygen (O_2) plasma, and Ozone (O_3) oxidization.[19,20]

D. Activation energy analysis

Temperature-dependent surface leakage (I_{surf}) and total leakage current current–voltage (I_{dark}) for a low TDD Ge PD with a 60 μm diameter are displayed in the temperature range from 293 to 353 K as a function of reverse bias from 0 to −3 V in Fig. 3(a). It is obvious that the extracted I_{surf} is close to I_{dark}, emphasizing again that the surface leakage current is the dominant leakage current component in such low TDD of 3.2×10^6 cm^{-2}. J_{dark} at −1 V was measured to be 3.96 mA/cm^2 at 293 K and increased by 3.1× at 323 K. Then, it reached 47 mA/cm^2 at 353 K, increasing 3.8× compared with the one at 323 K. J_{surf} at −1 V was extracted as 5.67 μA/cm at 293 K and increased by 3.1× at 323 K. Then, it reached 41.34 μA/cm at 353 K, increasing 2.4× compared with the one at 323 K. J_{bulk} was calculated by obtaining the subtraction of J_{dark} by J_{surf}. J_{bulk} was 0.16 mA/cm^2 at 293 K and increased by 2.2× at 323 K. Then, it reached 3.58 mA/cm^2 at 353 K, increasing 10.2× compared with the one at 323 K. It should be noted that a surface leakage variation is larger than that of a bulk leakage variation as the temperature is varied in a low-temperature region (293–323 K). On the other hand, in a high-temperature region (323–353 K), the bulk leakage variation in different operating temperatures is higher than that of the surface leakage variation.

In order to further investigate the leakage current mechanisms, it is necessary to study various leakage current mechanisms through the activation energy (E_a). E_a study is widely used to understand the leakage generation mechanisms in photodetectors. Leakage current generation mechanisms can be described by considering: (i) the diffusion leakage of carriers from neutral regions, (ii) the SRH leakage process, (iii) the TAT leakage process, and (iv) the tunneling of minority carriers through band-to-band tunneling (BTBT).[21] The diffusion leakage current has E_a of a material bandgap, ∼0.66 eV in the case of Ge. The SRH leakage current has E_a of half bandgap, ∼0.33 eV for Ge. The TAT leakage and BTBT leakage mechanisms have small E_a of <∼0.33 eV, below the half of Ge bandgap.

The SRH current density (J_{SRH}) and TAT current density (J_{TAT}) can be expressed by the following equations:

$$J_{SRH} + J_{TAT} = J_{SRH}(1 + \Gamma), \tag{2}$$

$$= \frac{qn_i W_d}{\tau_{eff}} = \frac{qn_i W_d}{\tau}(1 + \Gamma), \tag{3}$$

where Γ is the TAT enhancement factor and q, n_i, τ_{eff}, τ, and W_d are the electron charge, the intrinsic carrier concentration in Ge, the effective carrier lifetime, the SRH carrier lifetime, and the depletion width of Ge p-i-n diodes, respectively.[7] Γ has been

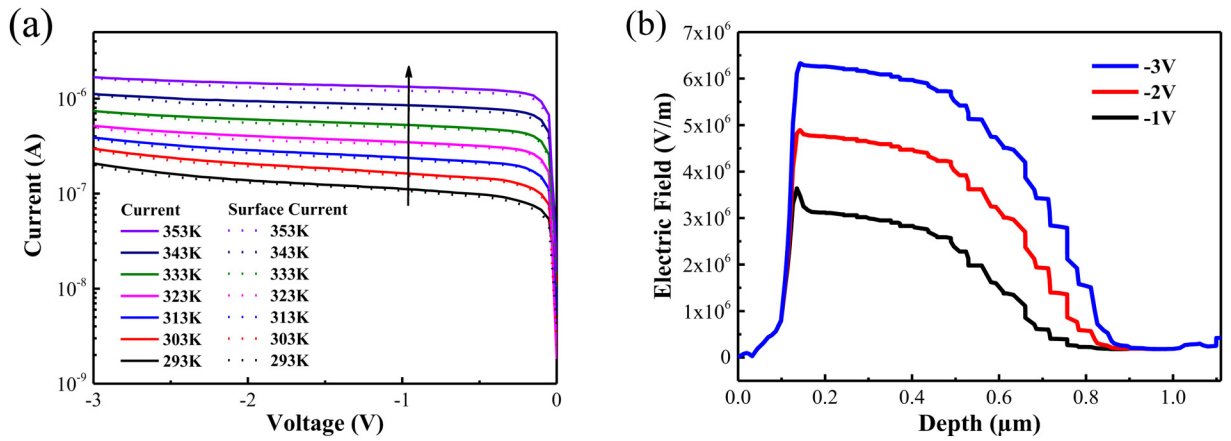

FIG. 3. (a) Temperature-dependent I_{dark} and I_{surf} for the low TDD Ge photodetector with 60 μm of a diameter in the temperature range of 293 to 353 K. The arrow represents the temperature increasing from 293 to 353 K. (b) Simulated electric field distribution for the low TDD Ge photodetector in the voltage range from −1 to −3 V.

introduced by Hurkx *et al.*[22] to describe the TAT process. Γ is affected by three parameters, i.e., tunneling effective mass, trap state energy, and the electric field in the depletion region. The decrease in temperature enhances the influence of Γ on the TAT process. In addition, a strong electric field and a small effective mass enhance Γ. Therefore, unlike other leakage current mechanisms, such as diffusion and SRH leakages that increase with temperature, TAT leakage can be enhanced by decreasing temperature, resulting from the increase in Γ.[10] This results in lower E_a than that of the SRH leakage process. The BTBT leakage current is strongly dependent on the electric field in the depletion region. The electric field distribution in a vertical *p-i-n* photodetector on a low TDD GOI substrate was simulated through Lumerical DEVICE simulation under various reverse bias, as shown in Fig. 3(b). The maximum electric field of $\sim 3 \times 10^6$ V/m is applied at −1 V and reaches $\sim 6 \times 10^6$ V/m at −3 V. The depletion region is formed near a n^+-mesa region and increases with the reverse bias. Based on the BTBT current equation described in Ref. 21, the BTBT current density at $\sim 6 \times 10^6$ V/m at −3 V is extremely low compared to the measured J_{dark}. It has been also reported that the BTBT leakage is dominant in a strong electric field of $>5 \times 10^8$ V/m in Ge junctions.[9] Therefore, BTBT leakage current contribution is negligible in this analysis.

Figure 4(a) displays the Arrhenius plot for low and high TDD Ge PDs as a function of $1/kT$ at −3 V under the temperature range of 293 to 353 K, where k is the Boltzmann constant. A non-linear relationship is observed in the Arrhenius plot for the low TDD Ge photodetector, while a linear relationship is observed for the high TDD Ge photodetector. The inset in Fig. 4(a) displays the Arrhenius plot for the extracted J_{surf} and J_{bulk} for low TDD Ge PDs. The corresponding E_a was extracted from the Arrhenius plot and is shown in Figs. 4(b)–4(d).

Figure 4(b) displays E_a for the high TDD Ge PD with a 250 μm diameter as a function of the operating voltage from −0.1

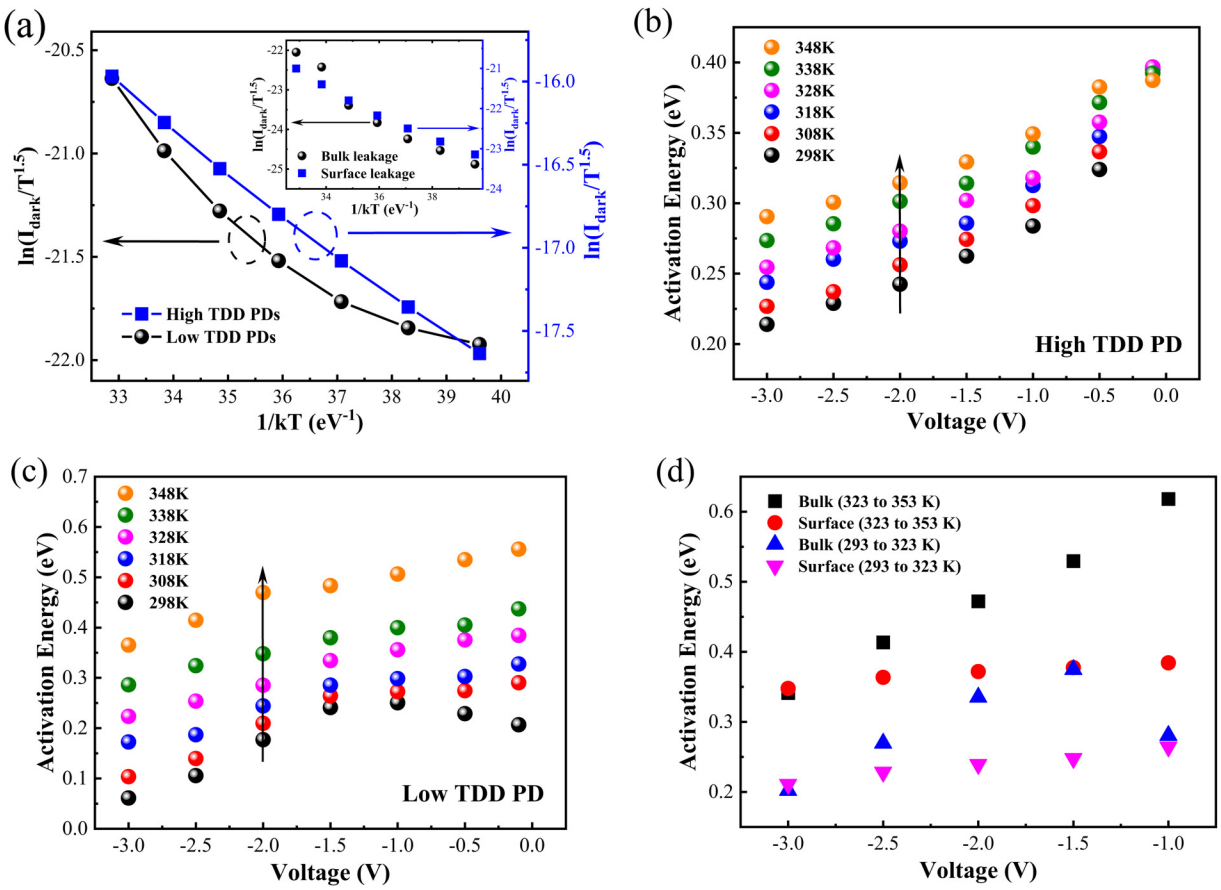

FIG. 4. (a) The Arrhenius plot for the low and high TDD photodetectors at −3 V. The inset displays the Arrhenius plot for bulk and surface leakage currents of the low TDD Ge photodetectors. Activation energy for (b) the high TDD Ge photodetector and (c) the low TDD Ge photodetector as a function of voltage of −0.1 to −3.0 V in the temperature range from 298 to 348 K. The arrows represent the temperature increasing from 298 to 348 K. Arrhenius plot of low TDD Ge photodetectors in various reverse applied voltage. (d) Activation energy for bulk and surface leakages for low TDD Ge photodetectors as a function of voltage from −0.1 to −3.0 V in high (293–323 K) and low (323–353 K) temperature.

to −3.0 V. As can be seen in Fig. 4(b), E_a at −0.1 V is ∼0.39 eV in the overall temperature range, representing that the leakage current is governed by the SRH process in low reverse bias. As the operating voltage increases to −3 V, E_a decreases to 0.21 at 298 K. This is because that the SRH process is enhanced by the TAT process in relatively high reverse bias. The E_a variation from 293 to 353 K at the reverse bias of −3 V is 0.08 eV, which originates from the temperature-dependent TAT leakage mechanism.[10]

Figure 4(c) displays E_a for the low TDD Ge photodetector with a 250 μm diameter as a function of an operating voltage of −0.1 to −3.0 V in the temperature range of 293–353 K. At a reverse voltage of −0.1 V, E_a of the low TDD Ge PD increases from 298 to 348 K. This can be explained that the SRH leakage mechanism with the TAT process is dominant at low temperature. As temperature increases, the dominant leakage mechanism of the low TDD Ge PD is converted to a diffusion leakage mechanism, which is different from that of the high TDD Ge PD. As TDD is reduced from 5.2×10^8 to 3.2×10^6 cm^{-2}, strong trap-dependent leakage mechanisms, such as SRH and TAT processes, are suppressed. Accordingly, the diffusion leakage, the non-trap-dependent leakage mechanism, appears as a favorable process. As reverse bias increases, E_a decreases and reaches 0.06 at 298 K at −3 V, supported by the fact that the TAT process is enhanced in a relatively high electric field. The E_a variations in different temperatures originate from strong temperature-dependent diffusion and TAT leakage mechanisms. E_a for the low TDD PD is widely spread in the overall temperature range (293–353 K) compared to that of high TDD Ge PDs. This is due to the alleviation of the SRH process, fundamentally originating from reduction in TDD. For the high TDD Ge PD, the leakage current is mainly contributed by SRH and TAT processes. However, since the SRH leakage mechanism is alleviated with the reduced TDD of 3.2×10^6 cm^{-2}, diffusion leakage should be favorably considered to interpret the leakage current mechanisms of the low TDD Ge PDs. Therefore, the diffusion and TAT process, which are temperature- and electric field-dependent, provide wide E_a variation for the low TDD Ge photodetectors.

In order to estimate the effectivity of the passivation layer of PECVD-deposited SiO_2, the E_a of the surface and bulk leakage currents of the low TDD Ge PDs are extracted separately in Fig. 4(d). E_a of the surface leakage current is 0.26 eV at a reverse voltage of −1 V in the low temperature (293–323 K). The E_a of surface current decreases to 0.2 eV as the reverse voltage increases to −3 V. This result indicates that the surface leakage current is dominated by SRH and TAT processes, which are related to surface states. In the high-temperature range, the E_a of bulk leakage current is as high as 0.61 eV at −1 V, implying diffusion leakage is dominant. The E_a of bulk leakage current decreases with the increase in reverse bias, indicating the TAT leakage process is considered as the primary mechanism in high reverse bias.

E. Effective lifetime analysis

In order to further understand the influence of TDD on Ge PDs, it is important to study the SRH and TAT leakage current mechanisms, which are widely reported as the primary leakage current processes. With the assumption that the diffusion length is longer than the depletion region, the information on the SRH and TAT leakages can be extracted by differentiating I_{dark} by W_d, as shown in the following equation:[9]

$$\frac{dI_{dark}}{dW_d} \approx \frac{dI_{diff}}{dW_d} + \frac{dI_{SRH} + dI_{TAT}}{dW_d} \approx \frac{qn_i}{\tau_{eff}}, \tag{4}$$

where I_{diff} is the diffusion leakage current. τ_{eff} provides the information on TDD-dependent lifetime of photodetectors. Since thicknesses of two different TDD Ge layers are different due to O_2 annealing and HF solution etching, τ_{eff} analysis could normalize the influence of TDD on SRH and TAT leakage processes. W_d for the low and high TDD Ge PDs was extracted through the capacitance–voltage (C–V) measurement in Fig. 5(a). The parasitic and the device capacitance can be extracted from the linear fitting of the capacitance as a function of photodetector mesa areas.[14] W_d for low TDD Ge PDs is thinner than that for high TDD Ge PDs, resulting from reduction in the Ge thickness by ∼300 nm during O_2 annealing and HF solution etching steps.

In order to extract τ_{eff}, n_i was referenced from Ref. 23, assuming that W_d is constant with temperature. Figure 5(b) displays τ_{eff} for the bulk leakage of low and high TDD Ge PDs as a function of reverse bias at 343 K. In the low reverse bias of −0.5 V, τ_{eff} for low and high TDD Ge PDs was extracted to be 5.7×10^{-7} and 2.9×10^{-9} s, respectively. τ_{eff} for low TDD Ge PDs is two orders of magnitude higher than τ_{eff} for the high TDD Ge PDs under overall reverse bias range of −0.2 to −3 V. We emphasize that the two orders of magnitude enhancement on the extracted τ_{eff} is corresponding to the two orders of magnitude reduction in TDD, confirming that τ_{eff} is significantly related to TDD.[24,25] τ_{eff} decreases with increasing reverse bias in Fig. 5(b). τ_{eff} reaches 4.8×10^{-8} and 2.2×10^{-10} s at −3.0 V for the low and high TDD Ge PDs, respectively. This is because that the strong electric field in the depletion region enhances Γ, resulting in the enhancement on the TAT leakage process.[10]

Temperature-dependent τ_{eff} of bulk leakage for low and high TDD Ge PDs at −1 V is displayed in Fig. 5(c). τ_{eff} for low TDD Ge PDs was extracted to be 1.9×10^{-7} s at −1 V at 293 K and increases to 4.9×10^{-7} s at 323 K. The τ_{eff} for the high TDD PD was extracted to be 5.0×10^{-10} s at −1 V at 293 K and increases to 1.4×10^{-9} s at 353 K. The increase in τ_{eff} with temperature originates from the suppressed TAT process. The TAT leakage process is alleviated by increasing temperature due to Γ, which is consistent with the E_a analysis. τ_{eff} for the bulk leakage of the low TDD PD is displayed as a function of temperature in the temperature range of 293–353 K in Fig. 5(d). The τ_{eff} is reduced from 1.9×10^{-7} to 7.5×10^{-9} s for −1 and −3 V, respectively, at 293 K. This is because that the TAT leakage process is enhanced in the relatively high electric field. The τ_{eff} at 353 K is reduced from 2.9×10^{-7} to 4.6×10^{-8} s for −1 and −3 V, respectively, as expected. At the same temperature, the τ_{eff} variation between −1 and −3 V decreases with increasing temperature, signifying that the TAT leakage is reduced by increasing temperature.[10]

Figure 6 represents a benchmarking of the reported SRH lifetime (τ) along with τ_{eff} for the low and high TDD Ge PDs. The modeling τ is calculated from Ref. 25. τ_{eff} reasonably matches well with modeling τ. Low TDD Ge τ_{eff} is enhanced by a factor of 185 compared with high TDD Ge τ_{eff}. It is worth noting that the

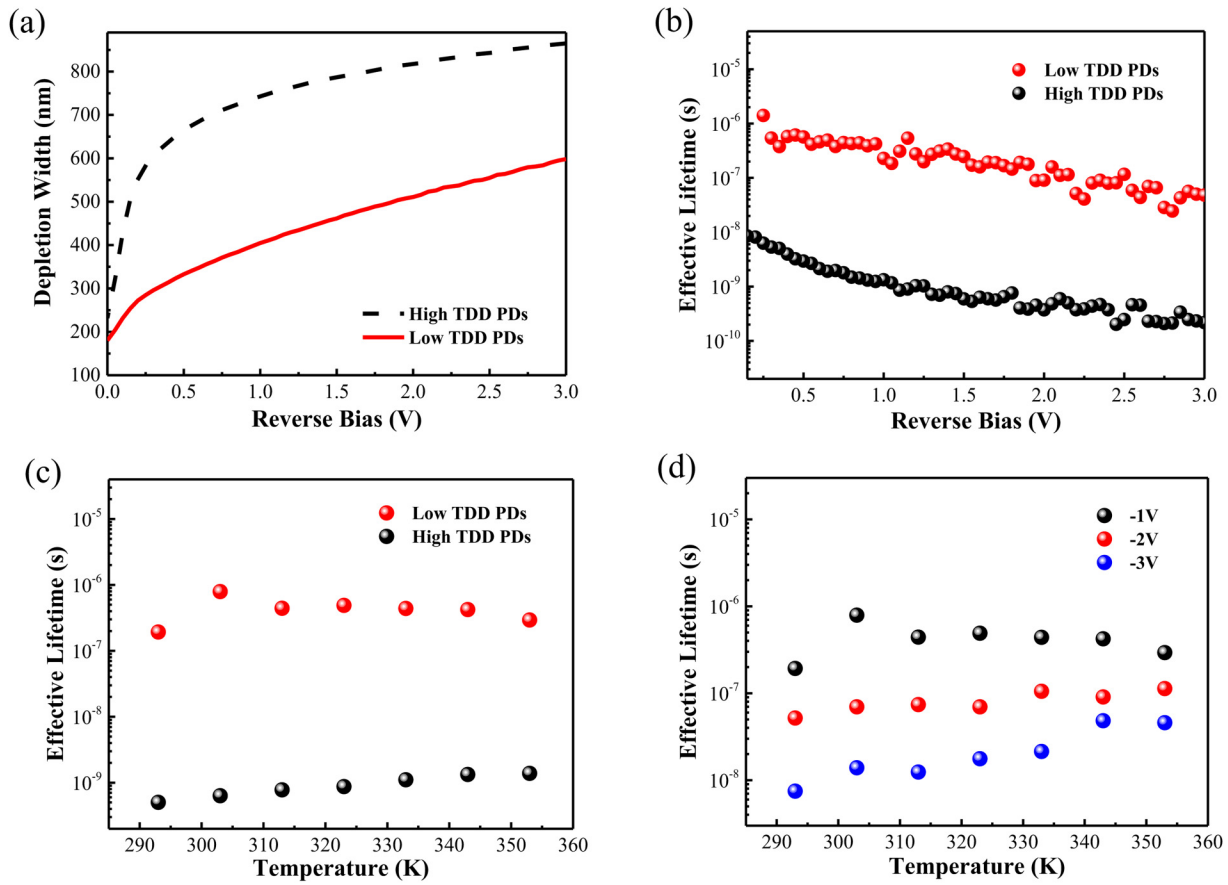

FIG. 5. (a) The depletion width for low and high TDD Ge photodetectors as a function of reverse bias. (b) The effective carrier lifetime for bulk leakage of low and high TDD Ge photodetectors as a function of reverse bias at 343 K. (c) The effective carrier lifetime for the bulk leakage of low and high TDD Ge photodetectors as a function of temperature. (d) The effective carrier lifetime for the bulk leakage of low TDD Ge photodetectors as a function of temperature under various operating voltages.

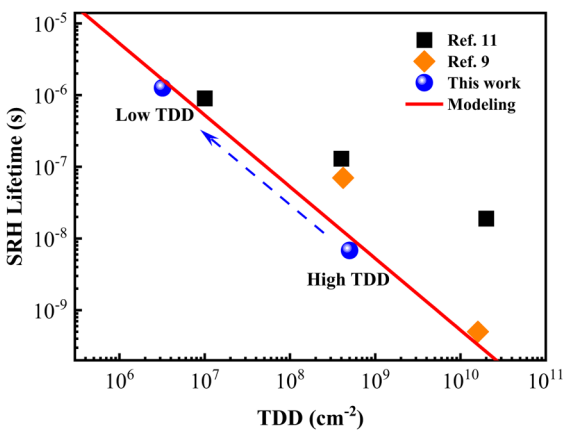

FIG. 6. Benchmarking of the SRH carrier lifetime for Ge p^+/n junctions and the effective carrier lifetime for the bulk leakage of low and high TDD Ge photodetectors.

185× enhancement in τ_{eff} is obviously consistent with 162× reduction in TDD, supporting the fact that τ_{eff} is reversely proportional to TDD.[24,25] In comparison with the J_{bulk} analysis, which provides the 374× reduction as TDD decreases, τ_{eff} analysis provides a better and direct interpretation of TDD in Ge films. Unlike τ_{eff} analysis that normalizes the effect of W_d, J_{bulk} is more sensitive to W_d.

III. CONCLUSION

A systematic dark current analysis of vertical *p-i-n* Ge photodetectors with two different TDDs, i.e., 3.2×10^6 and 5.2×10^8 cm^{-2}, respectively, was performed. J_{dark} for low TDD Ge photodetectors was achieved as 1.12 mA/cm^2, representing reduction by a factor of 53 from that of high TDD Ge photodetectors. The main leakage current contribution shifts from bulk leakage to surface leakage as TDD is reduced to 3.2×10^6 cm^{-2}. The surface leakage current contribution of 96% for the low TDD Ge photodetector shows that the advanced surface passivation is required to further reduce the dark leakage current. Through E_a analysis, it was confirmed that the bulk leakage for low TDD Ge photodetectors was governed by diffusion

leakage in the high-temperature region (323–353 K) at −1 V in contrast to full SRH leakage process dominance for high TDD Ge photodetectors. The surface leakage generated at the interface of PECVD-deposited SiO_2/Ge is governed by SRH and TAT leakage mechanisms in the temperature range of 293–353 K. τ_{eff} analysis was used to study the TDD-dependent carrier lifetime of photodetectors. τ_{eff} for the bulk leakage of low TDD Ge photodetectors was extracted to be 1.3×10^{-6} s, which is two orders of magnitude higher than τ_{eff} for high TDD Ge photodetectors. In this work, it was demonstrated that the bulk leakage density and τ_{eff} were significantly affected by the change in TDD.

ACKNOWLEDGMENTS

This work was supported by the National Research Foundation Singapore Competitive Research Programme under Grant No. NRF–CRP19–2017–01. We thank the Silicon-Center of Excellence for the use of optical measurement equipment.

DATA AVAILABILITY

The data that support the findings of this study are available from the corresponding author upon reasonable request.

REFERENCES

[1]D. Anh, C. Hong, J. Liu, W. Giziewicz, M. Beals, L. C. Kimerling, J. Michel, J. Chen, and X. Kärtner, "High performance, waveguide integrated Ge photodetectors," Opt. Express **15**(7), 3916–3921 (2007).
[2]L. Vivien, J. Osmond, J.-M. Fédéli, D. Marris-Morini, P. Crozat, J.-F. Damlencourt, E. Cassan, Y. Lecunff, and S. Laval, "42 GHz p.i.n germanium photodetectors integrated in a silicon-on-insulator waveguide," Opt. Express **17**(8), 6252–6257 (2009).
[3]M. Jutzi, M. Berroth, G. Wohl, M. Oehme, and E. Kasper, "Ge-on-Si vertical incidence photodiodes with 39-GHz bandwidth," IEEE Photonics Technol. Lett. **17**(7), 1510–1512 (2005).
[4]M. Verdun, G. Beaudoin, B. Portier, N. Bardou, C. Dupuis, I. Sagnes, R. Haïdar, F. Pardo, and J.-L. Pelouard, "Dark current investigation in thin P-i-N InGaAs photodiodes for nano-resonators," J. Appl. Phys. **120**, 084501 (2016).
[5]M. B. Gonzalez, E. Simoen, G. Eneman, B. D. Jaeger, G. Wang, R. Loo, and C. Claeys, "Defect assessment and leakage control in Ge junctions," Microelectron. Eng. **125**, 33–37 (2014).
[6]B. Son, Y. Lin, K. H. Lee, and C. S. Tan, "Dark current analysis of vertical p-i-n photodetectors on a germanium-on-insulator platform," in *2019 IEEE 16th International Conference on Group IV Photonics (GFP)* (IEEE, 2019), pp. 1–2.
[7]H. Chen, P. Verheyen, P. D. Heyn, G. Lepage, J. D. Coster, S. Balakrishnan, P. Absil, G. Roelkens, and J. V. Campenhout, "Dark current analysis in high-speed germanium p-i-n waveguide photodetectors," J. Appl. Phys. **119**, 213105 (2016).
[8]N. A. DiLello, D. K. Johnstone, and J. L. Hoyt, "Characterization of dark current in Ge-on-Si photodiodes," J. Appl. Phys. **112**, 054506 (2012).
[9]M. B. Gonzalez, G. Eneman, G. Wang, B. De Jaeger, E. Simoen, and C. Claeys, "Analysis of the temperature dependence of trap-assisted tunneling in Ge pFET junctions," J. Electrochem. Soc. **158**, H955–H960 (2011).
[10]E. Simoen, F. D. Stefano, G. Eneman, B. D. Jaeger, C. Claeys, and F. Crupi, "On the temperature and field dependence of trap-assisted tunneling current in Ge p^+n junctions," IEEE Electron. Device Lett. **30**(5), 562–564 (2009).
[11]G. Eneman, M. B. Gonzalez, G. Hellings, B. D. Jaeger, G. Wang, J. Mitard, K. D. Meyer, C. Claeys, and M. Heyns, "Trap-assisted tunneling in deep-submicron Ge PFET junctions," ECS Trans. **28**(5), 143–152 (2010).
[14]Y. Lin, K. H. Lee, S. Bao, X. Guo, H. Wang, J. Michel, and C. S. Tan, "High-efficiency normal-incidence vertical *p-i-n* photodetectors on a germanium-on-insulator platform," Photonics Res. **5**(6), 702–709 (2017).
[12]K. H. Lee, S. Bao, G. Y. Chong, Y. H. Tan, E. A. Fitzgerld, and C. S. Tan, "Defects reduction of Ge epitaxial film in a germanium-on-insulator wafer by annealing in oxygen ambient," APL Mater. **3**, 016102 (2015).
[13]Y. Wang, B. Wang, D. F. S. Eow, J. Michel, K. E. K. Lee, S. F. Yoon, E. A. Fitzgerald, C. S. Tan, and K. H. Lee, "Performance of AlGaInP LEDs on silicon substrates through low threading dislocation density (TDD) germanium buffer layer," Semicond. Sci. Technol. **33**, 104004 (2018).
[15]F. Suo, J. Tong, L. Qian, and D. H. Zhang, "Study of dark current in mid-infrared InAsSb-based hetero *n-i-p* photodiode," J. Phys. D Appl. Phys. **51**, 275102 (2018).
[16]X. Ma, Y. Huang, J. Fei, Q. Chen, T. Liu, K. Liu, X. Duan, X. Yan, and X. Ren, "Analysis of dark current considering trap-assisted tunneling mechanism for In GaAs PIN photodetectors," Opt. Quant. Electron. **49**, 407 (2017).
[17]S. Xu, W. Wang, Y.-C. Huang, Y. Dong, S. Masudy-Panah, H. Wang, X. Gong, and Y.-C. Yeo, "High-speed photo detection at two-micron-wavelength: Technology enablement by GeSn/Ge multiple-quantum-well photodiode on 300 mm Si substrate," Opt. Express **27**(4), 5798–5813 (2019).
[18]R. Zhang, T. Iwasaki, N. Taoka, M. Takenaka, and S. Takagi, "Al_2o_3/GeO_x/Ge gate stacks with low interface trap density fabricated by electron cyclotron resonance plasma pstoxidation," Appl. Phys. Lett. **98**, 112902 (2011).
[19]J. Kang, R. Zhang, M. Takenaka, and S. Takagi, "Suppression of dark current in GeO_x-passivated germanium metal-semiconductor-metal photodetector by plasma post-oxidation," Opt. Express **23**(13), 16967–16976 (2015).
[20]Y. Xu, G. Han, H. Liu, Y. Wang, Y. Liu, J. Ao, and Y. Hao, "Ge pMOSFETs with GeO_x passivation formed by ozone and plasma post oxidation," Nanoscale Res. Lett. **14**, 126 (2019).
[21]P. Chakrabarti, A. Gawarikar, V. Mehta, and D. Garg, "Effect of trap-assisted tunneling (TAT) on the performance of homojunction mid-infrared photodetectors based on InAsSb," J. Microwaves Optoelectron. **5**(1), 1–14 (2006).
[22]G. A. M. Hurkx, D. B. M. Klaassen, and M. P. G. Knuvers, "A new recombination model for device simulation including tunneling," IEEE Trans. Electron Devices **39**(2), 331–338 (1992).
[23]E. Simoen and J. Vanhellemont, "On the diffusion and activation of ion-implanted n-type dopants in germanium," J. Appl. Phys. **106**, 103516 (2009).
[24]N. S. Patel, "Understanding defects in germanium and silicon for optoelectronic energy conversion," Ph.D. dissertation (MIT, 2016).
[25]Y. Cai, "Materials science and design for germanium monolithic light source on silicon," Ph.D. dissertation (MIT, 2014).